Planta (2010) 231:1495–1504
DOI 10.1007/s00425-010-1148-3

ORIGINAL ARTICLE

Metabolic and structural rearrangement during dark-induced autophagy in soybean (*Glycine max* L.) nodules: an electron microscopy and ^{31}P and ^{13}C nuclear magnetic resonance study

Pierre Vauclare · Richard Bligny · Elisabeth Gout · Valentine De Meuron · François Widmer

Received: 21 December 2009 / Accepted: 26 February 2010 / Published online: 1 April 2010

Abstract The effects of dark-induced stress on the evolution of the soluble metabolites present in senescent soybean (*Glycine max* L.) nodules were analysed in vitro using ^{13}C- and ^{31}P-NMR spectroscopy. Sucrose and trehalose were the predominant soluble storage carbons. During dark-induced stress, a decline in sugars and some key glycolytic metabolites was observed. Whereas 84% of the sucrose disappeared, only one-half of the trehalose was utilised. This decline coincides with the depletion of Gln, Asn, Ala and with an accumulation of ureides, which reflect a huge reduction of the N_2 fixation. Concomitantly, phosphodiesters and compounds like P-choline, a good marker of membrane phospholipids hydrolysis and cell autophagy, accumulated in the nodules. An autophagic process was confirmed by the decrease in cell fatty acid content. In addition, a slight increase in unsaturated fatty acids (oleic and linoleic acids) was observed, probably as a response to peroxidation reactions. Electron microscopy analysis revealed that, despite membranes dismantling, most of the bacteroids seem to be structurally intact. Taken together, our results show that the carbohydrate starvation induced in soybean by dark stress triggers a profound metabolic and structural rearrangement in the infected cells of soybean nodule which is representative of symbiotic cessation.

Keywords Peribacteroid membrane · Glycine · Metabolic NMR · Nodules · Senescence

Abbreviations

Fru6P	Fructose 6-phosphate
GABA	γ-Aminobutyric acid
Glc6P	Glucose 6-phosphate
Glyc3P	Glycerol 3-phosphate
GPC	Glycerylphosphoryl-choline
GPE	Glycerylphosphoryl-ethanolamine
GPG	Glycerylphosphoryl-glycerol
GPI	Glycerylphosphoryl-inositol
Man6P	Mannose 6-phosphate
PBM	Peribacteroid membrane
P-cho	Phosphoryl-choline
P-eth	Phosphoryl-ethanolamine
SEM	Scanning electron microscopy
TEM	Transmission electron microscopy

Introduction

Legumes play an important role in agricultural food production (Doyle and Luckow 2003). Among them, soybean (*Glycine max*) is a major crop cultivated for oil and protein production. Like other legumes, soybean develops specialised root organs, called nodules, in which host cells establish a symbiotic association with rhizobia (Perret et al.

Electronic supplementary material The online version of this article (doi:10.1007/s00425-010-1148-3) contains supplementary material, which is available to authorized users.

P. Vauclare · V. De Meuron · F. Widmer
Laboratory of Plant Biology and Physiology,
Biology Building UNIL, room 5449,
1015 Lausanne, Switzerland

R. Bligny · E. Gout
Laboratoire de Physiologie Cellulaire Végétale,
Unité Mixte de Recherche 5168, Institut de Recherche
en Technologie et Sciences pour le Vivant CEA,
17, rue des Martyrs, 38054 Grenoble Cedex 9, France

Present Address:
P. Vauclare (✉)
22, rue du Lavoir, 26120 Malissard, France
e-mail: pierre.vauclare@wanadoo.fr

2000; Broughton 2003). Differentiated bacteria, called bacteroids, express the nitrogenase enzyme complex, which reduces atmospheric nitrogen (N_2) to ammonia at the expense of 16 ATP per mol of N_2. Ammonia is then supplied to the host cells and converted into organic compounds (amides or ureides), which are exported to the shoots (for a review, see Tajima et al. 2004). In return, leaves deliver carbohydrates into the nodules via the phloem to provide the energy required for N_2 fixation (for a review see Schubert 1986; Prell and Poole 2006). Because this symbiotic relationship is the largest source of available nitrogen on earth, culture of legumes reduces the need for expensive fertilizers, reducing the pollution of the ecosystem (Newton 2000). The active period of N_2 fixation is limited during nodule development because nodule senescence occurs rapidly after flowering and during seed maturation (Espinosa-Victoria et al. 2000; Puppo et al. 2005). This senescence is also observed in leguminous plants in response to environmental perturbations like drought, low temperature, defoliation, external addition of nitrogen and pathogenic attack (Cots et al. 2002; Patriarca et al. 2004; Puppo et al. 2005). In addition, nodule senescence can be artificially triggered by exposing soybean plants to prolonged darkness (Cohen et al. 1986; Gordon et al. 1993; Fargeix et al. 2004). Although dark-induced senescence is a premature phenomenon, it shares many of the molecular, physiological and ultrastructural characteristics found in naturally senescing nodules, such as the loss of nitrogenase activity, the increase in proteolytic activity and the greenish colour of nodule tissues (Pfeiffer et al. 1983; Cohen et al. 1986; Jacobi et al. 1994; Fargeix et al. 2004). Because natural senescence is an irreversible phenomenon, understanding the physiological processes which occur during induced senescence could help to find strategies that delay this phenomenon and extend the active period of rhizobium–plant symbiosis (Espinosa-Victoria et al. 2000). Recently, a transcriptomic study has been performed on the senescence of indeterminate nodules in *Medicago truncatula* (Van de Velde et al. 2006). During this complex process a wide variety of defence and stress-response genes are transcribed in senescing *M. truncatula* nodules, an event which is marked by the transition of the nodule from a carbon sink to a general nutrient source (Van de Velde et al. 2006). Interestingly, although determinate (soybean) and indeterminate nodule types show a very different anatomical structure, which makes comparison with their senescing physiological responses difficult (Puppo et al. 2005), some quite common modifications have been observed. One of the main events was observed in soybean as well as in *M. truncatula* using transmission electron microscopy (TEM). It concerns the alteration of the structure of the symbiosomes, an organelle-like compartment in which bacteroids are surrounded by a specialised membrane called the peribacteroid membrane (Fargeix et al. 2004; Van de Velde et al. 2006). However, while this alteration is considered as the earliest observable event associated with a loss of nitrogen-fixing activity, little information is available on the metabolic modifications during nodule senescence in soybean (Cohen et al. 1986; Fargeix et al. 2004; Van de Velde et al. 2006). For these reasons, we performed further experiments to demonstrate unambiguously the autophagic process in relation to the down-regulation of the nitrogen metabolism. This prompted us to draw up the metabolite profile to characterise some easily identifiable marker(s) of autophagy and peribacteroid membrane (PBM) evolution in senescing soybean nodules by using in vitro ^{13}C- and ^{31}P-nuclear magnetic resonance spectroscopy, scanning electron microscopy (SEM) and biochemical measurements.

Materials and methods

Plant materials and growth conditions

Soybean seeds (*Glycine max* L., var Mapple arrow; Schweizer Samen AG, Thoune, Switzerland) were thoroughly washed in water, incubated for 20 min at 42°C and then washed a second time in water. The swollen seeds were then transferred into a mixture of vermiculite and potting soil (Triohum; Mauser Samen, Winterthur, Switzerland) without fertilizer [1:1]. Plants were grown in a greenhouse under controlled conditions with a light phase of 16 h, and temperatures of 20°C (day) and 18.5°C (night).

Bradyrhizobium japonicum (strain 110, spc 4, wild type) was grown in sterilised liquid culture [4% bactopeptone (p/v), 1 mM KH_2PO_4, 2 mM $MgSO_4{\cdot}7H_2O$, pH 6.8] with spectinomycine (100 µg/ml) for 6 days at 28°C. Centrifuged bacteria were diluted in phosphate-buffered saline medium (0.14 M NaCl, 2.5 mM KCl, 4 mM Na_2HPO_4, 2 mM KH_2PO_4, pH 7.4). Seven days after imbibition, each plant was inoculated with 10^8–10^9 *B. japonicum* strain. One week after infection, a fertilizer (Basisdünger Hauert-Flory, Grossaffoltern, Switzerland) was added and this was repeated once a week; 28–32 days of growth after inoculation were required to obtain mature nodules. For the experiments, 30-day-old plants were placed in darkness or under normal growth conditions for 4, 7, 11 and 14 days.

In vitro NMR spectroscopy

Perchloric acid (PCA) extracts were prepared from 8 g of fresh nitrogen frozen soybean nodules according to the method described by Gout et al. (2000). Spectra of neutralised PCA extracts were obtained on an NMR spectrometer (AMX 400, Bruker, Billeria, MA, USA) equipped with a 10-mm multinuclear probe tuned at 162 or 100.6 MHz for

^{31}P- or ^{13}C-NMR studies, respectively. The deuterium resonance of D_2O (100 µl added per millilitre of extract) was used as a lock signal.

Conditions used for ^{13}C-NMR acquisition were as follows: 90° radio-frequency pulses (19 µs) at 6 s intervals; spectral width, 20,000 Hz; 900 scans; and Waltz-16 ^{1}H decoupling sequence (with two levels of decoupling: 2.5 W during acquisition time, 0.5 W during delay). Free induction decays were collected as 16,000 data points, zero filled to 32,000 and processed with a 0.2-Hz exponential line broadening. The ^{13}C-NMR spectra are referenced to hexamethyldisiloxane at 2.7 ppm. Mn^{2+} ions were chelated by the addition of 2 µM 1,2-cyclohexylenedinitrilotetraacetic acid (CDTA) and the pH was adjusted to 7.5 (sample volume 2.5 ml). The spectra of nodules were compared with the spectra of a PCA extract of sycamore cells.

The conditions used for ^{31}P-NMR acquisition were as follows: 70° radio-frequency pulses (15 µs) at 3.6 s intervals; spectral width 8,200 Hz; 1,024 scans; Waltz-16 ^{1}H decoupling sequence (with two levels of decoupling: 1 W during acquisition time, 0.5 W during delay). Free induction decays were collected as 8,000 data points, zero filled to 16,000 and processed with a 0.2-Hz exponential line broadening. The ^{31}P-NMR spectra were referenced to methylene diphosphonic acid, pH 8.9, at 16.38 ppm. Before ^{31}P-NMR analyses, divalent paramagnetic cations (Ca^{2+}, Mg^{2+}, Mn^{2+}, etc.,) were chelated by addition of appropriate amounts of CDTA ranging from 100 to 150 µM (sample volume of 2.5 ml). The pH was buffered by the addition of 75 µmol Hepes and adjusted to 7.5. Identified compounds were quantified by comparison of the areas of their resonance peaks with those of known amounts of maleate and methylphosphonate as internal standards for ^{13}C- and ^{31}P-NMR analyses, respectively.

Scanning electron microscopy

Samples were frozen in liquid N_2, fragmented, and then fixed overnight in 2% OsO_4 and 3% CrO_3 at room temperature. Dehydration was carried out on ice by successive 10 min incubations in 30, 50, 70, 80, 90 and 100% acetone solutions, and samples were stored at −20°C. A critical drying (Critical Point Dryer, Baltec-Leica Microsystems, Wetzlar, Germany) was performed, followed by coating with gold for 3 min, and samples were observed with a Jeol JSM-6300F (Tokyo, Japan) microscope at an accelerating voltage of 5 kV.

Isolation of peribacteroid membranes (PBM) from soybean nodules

Membrane fractions were prepared as described by Bassarab et al. (1989) with slight modifications. Fresh nodules (4–8 g) stocked overnight at 4°C (Day et al. 1987) were crushed, using a chilled mortar and pestle, in 10 ml of cold buffer containing 75 mM Tris/HCl at pH 7.5, 10 mM KCl, 1 mM $MgCl_2$, 1 mM EDTA, 1 mM phenylmethylsulfonyl fluoride (PMSF), 2 mM 1,4-dithioerythritol (DTT) and 12% sucrose. The crushed material was filtered through three layers of moist Miracloth, and then centrifuged for 10 min at 750*g*. The supernatant was transferred to the top of a continuous sucrose gradient (24 ml of 60–30% sucrose which in turn was layered over 5 ml of 20% sucrose) and centrifuged for 2 h at 90,000*g*. Fractions corresponding to various cell compartments were identified by using the following marker enzymes: alcohol dehydrogenase, NADH cytochrome-*c* reductase and cytochrome-*c* oxidase for cytosol, endoplasmic reticulum, and mitochondria, respectively (Quail 1979; Lord 1987; Lee et al. 1995).

The band of peribacteroid units (PBUs) or symbiosomes were collected, adjusted to 20% sucrose with a buffer (5 mM Tris/HCl, pH 7.5, 1 mM EDTA, 1 mM PMSF, 2 mM DTT), and centrifuged for 30 min at 6,000*g*. The pellet was re-suspended in 6 ml of 6% sucrose; PBUs were pressed 10 times through a hypodermic needle (0.6 × 30 mm, Microlance 3), and the suspension was transferred to the top of 10 ml of 35% sucrose and centrifuged for 30 min at 50,000*g*. The identification of PBM fraction was identified by immunodetection using a nodulin-26 (NOD 26) antibody with a procedure described by Weaver et al. (1991). The interface containing PBM was recovered, adjusted to 6% sucrose in buffer (5 mM Tris/HCl, pH 7.5, 1 mM EDTA, 1 mM PMSF, 2 mM DTT) and centrifuged for 30 min at 50,000*g*. The PBM was recovered from the pellet and diluted in 1 ml of a buffer containing 25 mM Tris–Mes at pH 6.5, 0.25 M sucrose, 1 mM DTT and 20% glycerol. Samples were stored at −20°C after saturation with N_2.

Quantification of fatty acid

Lipids from frozen PBM were extracted by the method of Bligh and Dyer (1959). To measure fatty acids, phospholipids were transesterified according to Bassarab et al. (1989). Myristic acid (14:0) was used as an internal standard. Methyl-ester derivates were analysed on a Hewlett-Packard 5890 gas chromatograph [SP TM-2330 glass column from Supelco (Sigma-Aldrich, Buchs, Switzerland) 30 m long × 0.75 mm i.d., 0.2 µm film thickness] equipped with a flame ionisation detector and an automatic data analysis. Programme conditions were as follows: from 100 to 160°C (25°C min^{-1}), from 160 to 200°C (8°C min^{-1}) and finally 220 to 100°C (25°C min^{-1}).

Results

Metabolite profiling of soybean nodules' cells

In vitro ^{13}C- and ^{31}P-NMR spectroscopy from perchloric acid (PCA) extracts was performed to obtain the metabolic profile of 41-day-old soybean nodules infected with *B. japonicum* (Fig. 1a, Table 1). Among the different resonance signals detected by ^{13}C-NMR (Table 1), the highest corresponded to the ^{13}C of D-*chiro*-inositol and *myo*-inositol, the two major polyols present in soybean nodules [8.6 μmol g^{-1} fresh weight (FW)] (Streeter 1987). The other major resonances observed correspond to those of the carbons of sucrose (5.78 μmol g^{-1} FW) and trehalose (4.2 μmol g^{-1} FW), a non-reducing disaccharide sugar restricted to root nodules (Table 1). As expected, malate (0.625 μmol g^{-1} FW) was also detected at high concentrations (Table 1), as this dicarboxylic acid is efficiently respired by nodule host cells and bacteroids to support N_2 fixation (Day and Copeland 1991; Lodwig and Poole 2003). One of the main amino acids detected was asparagine (6.1 μmol g^{-1} FW), which is two to three times higher than the ureides (allantoin and allantoic acid) and glutamate (Table 1). There were also two smaller signals emerging from the background noise: γ-aminobutyric acid (GABA; 0.78 μmol g^{-1} FW) and alanine (0.94 μmol g^{-1} FW) (Table 1). Finally, glutamine signals are almost undetectable (0.63 μmol g^{-1} FW) suggesting a high turnover of this amino acid (Table 1). The ^{31}P-NMR spectra showed that the major compound was the inorganic phosphate (Pi; 7.1 μmol g^{-1} FW; Fig. 1a; Table 1). The presence of signals corresponding to sugar phosphates [glucose 6-phosphate (Glc6P), fructose 6-phosphate (Fru6P), 3-phosphoglycerate (PGA) and dihydroxyacetone-phosphate (DHAP)] reflects the glycolytic pathway activity. The precursor of ascorbate biosynthesis, mannose 6-phosphate (Man6P), was also found to accumulate in nodules (Wheeler et al. 1998; Matamoros et al. 2006) (Fig. 1a, Table 1). Nucleoside diphosphate sugars such as UDP-glucose (UDP-Glc), UDP-galactose (UDP-Gal) and UDP-N-acetylglucosamine (UDP-GlcNAc) were also detected. Contrary to UDP-Glc, UDP-Gal and UDP-GlcNAc were present only at trace levels. Intermediates in the synthesis and hydrolysis of phospholipids like phosphoryl-choline (P-cho) and phosphoryl-ethanolamine (P-eth) and phosphodiesters glycerylphosphoryl-choline (GPC) and glycerylphosphoryl-inositol (GPI) were identified (Fig. 1a, Table 1). Among nucleotides, UTP (0.07 μmol g^{-1} FW) was about twice as high as ATP. The low ATP concentration compared with that of AMP (0.88 μmol g^{-1} FW, Fig. 1a, Table 1) is typical of a hypoxic metabolism. Finally, we observed the presence of significant amounts of pyridine nucleotides, mainly NAD and NADPH. In contrast, NADP$^+$ was not detected,

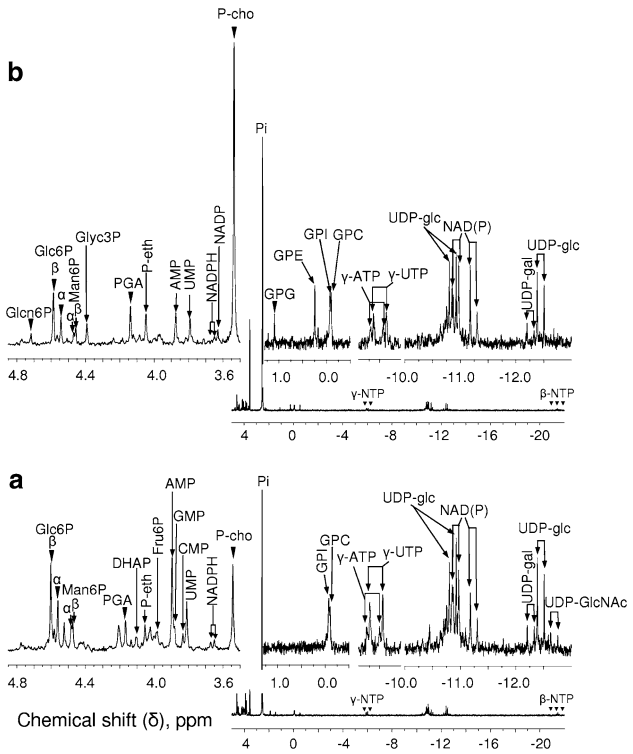

Fig. 1 Representative in vitro ^{31}P-NMR spectra of excised soybean nodules from 30-day-old plants subsequently kept under normal culture condition for 11 days (**a**) or kept in total darkness for 11 days (**b**). Extracts were prepared from 8 g of nodules (on a fresh weight basis) and analysed by ^{31}P-NMR. DHAP, dihydroxyacetone-phosphate; Fru6P, fructose 6-phosphate; Glcn6P, gluconate 6-phosphate; Glc6P, glucose 6-phosphate; Glyc3P, glycerol 3-phosphate; Pi, inorganic phosphate; Man6P, mannose 6-phosphate; PGA, 3-phosphoglycerate; P-eth, phosphoryl-ethanolamine; P-cho, phosphoryl-choline; UDP-glc, UDP-glucose; UDP-gal, UDP-galactose; UDP-GlcNAc, UDP-N-acetylglucosamine

which suggests that the reducing power coupled to the pentose phosphate pathway (Hong and Copeland 1990) is active in nodules under our culture conditions.

Effects of dark stress on metabolic profiling of nodules

Nodules taken from 30-day control soybeans after a 11-day dark treatment showed important metabolic changes that could mimic natural senescence at the physiological level (Fig. 1b, Table 1). A major observation from the ^{13}C-NMR spectra is that sucrose (0.93 μmol g^{-1} FW) was reduced by 84% during dark stress, whereas the corresponding decrease in trehalose was only 48% (2.18 μmol g^{-1} FW, Table 1). Inositol remained stable during the 11 days of darkness. Interestingly, whereas amino acids' spectra of glutamine, glutamate, alanine and asparagine presented a marked decrease in their amounts; a three- to fivefold increase in allantoate (5.93 μmol g^{-1} FW) and allantoin (5.16 μmol g^{-1} FW) levels was observed (Table 1). However,

Table 1 Effect of prolonged dark stress of soybean plants on the metabolite contents of nodules

Metabolites	Nodule (*Glycine max*)	
	Control	Dark
Sucrose	5.78 ± 1.16	0.93 ± 0.19*
Trehalose	4.2 ± 0.84	2.18 ± 0.43*
Inositol	8.6 ± 1.72	8.6 ± 1.72
Glu	2.18 ± 0.43	n.d.*
Gln	0.63 ± 0.13	n.d.*
Asn	6.1 ± 1.22	3.13 ± 0.63*
Ala	0.94 ± 0.19	n.d.*
Aln	1.1 ± 0.22	5.16 ± 1.03*
Alac	1.9 ± 0.38	5.93 ± 1.19*
Malate	1.56 ± 0.31	n.d.*
GABA	0.78 ± 0.16	1.25 ± 0.25*
Choline	n.d.	3.3 ± 0.65*
Pi	7.1 ± 0.99	8.1 ± 1.13
Glcn6P	n.d.	0.09 ± 0.01*
Glc6P	1.25 ± 0.18	0.7 ± 0.1*
Man6P	0.25 ± 0.03	0.14 ± 0.02*
Glyc3P	n.d.	0.18 ± 0.025*
PGA	0.27 ± 0.04	0.36 ± 0.05
Fru6P	0.16 ± 0.022	n.d.*
DHAP	0.11 ± 0.015	n.d.*
P-cho	0.8 ± 0.11	2.7 ± 0.4*
P-eth	0.23 ± 0.03	0.29 ± 0.04
GPG	n.d.	0.071 ± 0.01*
GPE	n.d.	0.15 ± 0.02*
GPI	0.13 ± 0.02	0.14 ± 0.02
GPC	0.11 ± 0.015	0.13 ± 0.02
UDP-Glc	1.02 ± 0.15	0.8 ± 0.1*
UDP-Gal	0.11 ± 0.015	0.07 ± 0.01*
UDP-GlcNAc	0.09 ± 0.013	n.d.*
AMP	0.88 ± 0.12	0.27 ± 0.037*
GMP	0.2 ± 0.03	n.d.*
CMP	0.14 ± 0.02	n.d.*
UMP	0.45 ± 0.06	0.22 ± 0.03*
UTP	0.18 ± 0.03	0.1 ± 0.014
ATP	0.07 ± 0.01	0.05 ± 0.007
NADP	n.d.	0.1 ± 0.014*
NADPH	0.13 ± 0.018	0.02 ± 0.003*
NAD	0.32 ± 0.045	0.24 ± 0.034

Metabolites were determined from perchloric acid (PCA) extracts, using maleate and methylphosphonate as internal standards for ^{13}C- and ^{31}P-NMR analyses, respectively. Values are expressed in μmol g^{-1} FW. Abbreviations of phosphorylated compounds are as in caption of Fig. 1. *Ala* alanine, *Aln* allantoin, *Alac* allantoate, *Asn* asparagine, *Glu* glutamate, *Gln* glutamine, *GABA* γ-aminobutyric acid. Results are given as mean ± SD (n = 3). nd, not detected

* Dark stress values significantly different from those of the control

the asparagine signals emerged clearly from the background noise (3.13 μmol g^{-1} FW). Concerning the pool of GABA, its concentration doubled in the dark-treated sample to reach 1.25 μmol g^{-1} FW, whereas malate was below the threshold of ^{13}C-NMR detection. Of particular interest was the detection of two intermediates implicated in membrane lipid synthesis in stressed nodules, P-cho (peaks at 57.77, 54.73 and 54.69 ppm) and free choline (peaks at 54.66, 54.62 and 54.58 ppm) corresponding to the three methyl groups coupled to the N atom of these molecules. Using ^{31}P-NMR spectroscopy, we observed that in dark-treated root nodules, P-cho became the major phosphorylated compound (2.7 μmol g^{-1} FW) whereas P-eth increased only slightly (Fig. 1b, Table 1). A new peak corresponding to glycerol 3-phosphate (Glyc3P) was detected. The accumulation of P-cho and Glyc3P reveals a membrane hydrolytic process (Dorne et al. 1987; Roby et al. 1987; Aubert et al. 1996). Moreover, two new phosphodiesters corresponding to glycerylphosphoryl-glycerol (GPG) and glycerylphosphoryl-ethanolamine (GPE) were detected. The other phosphorylated compounds, including Glc6P and Man6P, the major sugar phosphate compounds, UDP-Glc and UDP-Gal decreased significantly, whereas UDP-GlcNAc, Fru6P and DHAP became undetectable (Fig. 1b, Table 1). Interestingly, we found at 4.72 ppm a new peak corresponding to Glcn6P, a hexose-P involved in the pentose phosphate pathway (PPP) and in the regeneration of NADPH (Hong and Copeland 1990; Anthon and Emerich 1990). Finally, we observed a decrease in the total amount of soluble NTP. This was accompanied by a collapse in the content of NMP (Fig. 1b, Table 1). We conclude that a long period without photosynthesis induces important changes in the metabolite profile of root nodules in soybean related to an autophagy process. Since nodules contain a high proportion of symbiotic rhizobia surrounded by a PBM, we hypothesised that this PBM is particularly affected in senescing nodules. In order to test this hypothesis, we examined the fate of PBM during dark stress by SEM and a biochemical approach.

Ultrastructural effects of senescence on soybean nodules

Scanning electron microscopy was used to study the ultrastructural changes of infected cells in mature nodules during prolonged darkness. As shown in Fig. 2a and b, three-dimensional observation reveals a central part of the nodules containing cells infected or not. Infected cells in control nodules present hundreds of symbiosomes in which bacteroids were enclosed in an intact PBM (Fig. 2b). The external structure of symbiosomes corresponds to the PBM and looks like a big stick (Fig. 2c, d). We observed after

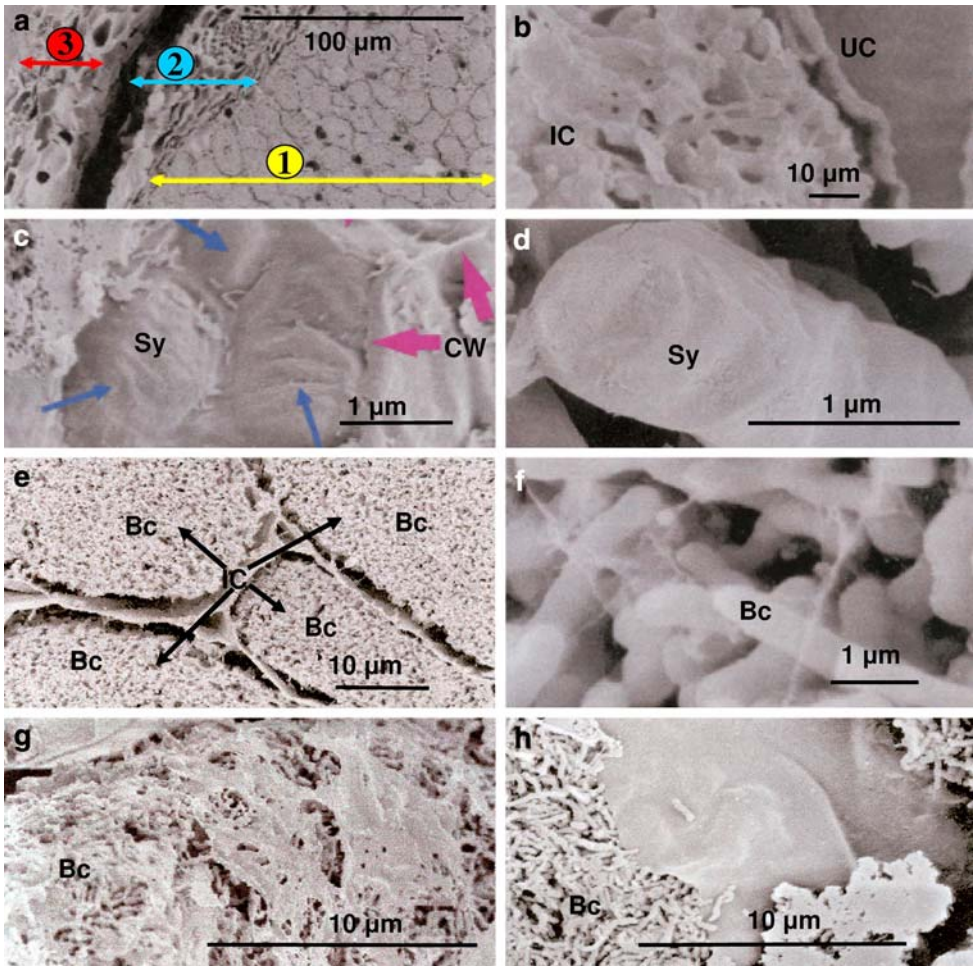

Fig. 2 Scanning electron micrographs of nodule sections of soybean 30 days post-inoculation **(a–d)** and of plants kept in darkness for 11 days **(e–h)**. **a** Area 1, central zone; 2, subcortex; 3, collapsed cells of exogenous cortex. **b** IC, infected cells; UC, uninfected cells. **c**, **d** CW, cell wall (→); Sy, intact symbiosomes. **e**, **f** Free bacteroids (Bc) in infected cells (IC). **g**, **h** Degeneration of membranes. Bc: bacteroids

11 days of dark treatment that some infected cells were filled with free bacteroids (Fig. 2e, f). Indeed, a disruption of membranes was observed, and bacteroids were released owing to the complete digestion of PBM (Fig. 2g, h). As shown in Fig. 2f, bacteroids are homogenous and rod-shaped, in contrast to the different shapes (oval or round) generally observed by TEM (Cohen et al. 1986; Fargeix et al. 2004). Moreover, we observed that some symbiosomes were going to merge (data not shown). Andreeva et al. (1998) made the same observation on senescing soybean, showing that some PBMs merge together to form large symbiosomes with an average of 20–30 bacteroids inside.

Biochemical changes of nodular peribacteroid membrane fatty acid content

Symbiosomes were isolated from mature soybean nodules infected with *B. japonicum*. They distinctly sediment (density: 1.25) from the other cell compartments. Afterwards, they were fractionated and the PBM was separated from the bacteroids. To confirm that the isolated fraction corresponds to the PBM, nodulin-26 protein (NOD 26), a typical marker for symbiosome membranes, was detected by using Western blot analysis according to Miao and Verma (1993) (data not shown). The absence (<1%) of cytochrome-*c* oxidase activity (an enzyme located in the inner mitochondrial membrane) in the PBM fraction indicates that the PBM was devoid of contamination by other membranes. The fatty acids of purified soybean PBM were then analysed by gas chromatography. Figure 3a and Table 2 show a typical plant fatty acid composition with saturated (16:0, palmitic acid; 18:0, stearic acid) and unsaturated fatty acids ($16{:}1^{\Delta 3trans}$, palmitic acid; $18{:}1^{\Delta 9cis}$, oleic acid; $18{:}2^{\Delta 9,12}$, linoleic acid and $18{:}3^{\Delta 9,12,15}$, α-linolenic acid). Linoleic acid and palmitic acid are the two major fatty acids (Fig. 3a, Table 2). Whereas linoleic acid was considered by Bassarab et al. (1989) as the principal PBM fatty acid in soybean nodules, it was however palmitic acid which predominated in our experiments on mature soybean nodules (Fig. 3a, Table 2).

After 6 weeks of growth, soybean plants were stressed by placing half of them in the dark. The PBM fatty acid composition was then regularly analysed over 14 days in treated (dark) and untreated nodules (light) (Fig. 3a, b; Table 2). Dark treatment of nodules leads to a decrease in

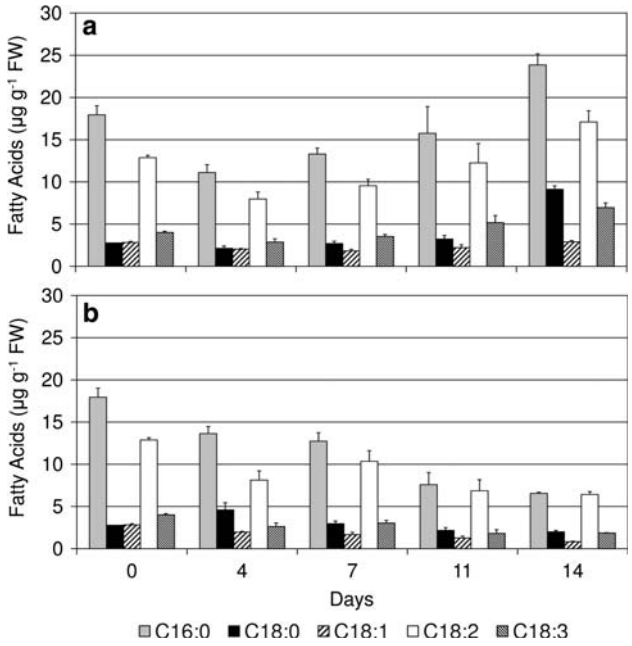

Fig. 3 Evolution of PBM fatty acid composition from 30-day-old soybean plants. **a** Plants kept under normal condition**. b** Plant kept under dark treatment at five different stages of development (0, 4, 7, 11 and 14 days). Fatty acid concentrations were quantified by GC using myristic acid as internal standard. Values represent the means ± SD ($n = 3$). 16:0, palmitic acid; 18:0, stearic acid; 18:1, oleic acid; 18:2, linoleic acid and 18:3, linolenic acid

total PBM fatty acid concentration (Fig. 3b). A significant drop was observed after 7 days of darkness, whereas untreated nodules show an increase in the total fatty acid concentration as further as 14 days from the beginning of the experiment (Fig. 3a, b). These results were closely related to an increase in the amount of total free fatty acids which trebled after 4 days of dark treatment [0.4 mg/g FW: control; 1.2 mg/g FW: 4 day dark (DD)] to reach 1.4 mg/g FW after 14 days of senescence. The PBM fatty acid composition showed a general decrease of each fatty acid from soybean plants kept in darkness for 11 and 14 days (Fig. 3b). Palmitic and linoleic acids seem to be particularly affected. However, if we compare the ratio of C18-unsaturated to C16- and C18-saturated fatty acids during the course of the experiment in dark stress nodules, no significant variations to the control value were observed (Table 2). In addition to these observations, we followed the evolution of phospholipid concentrations. A fall of 43% of phospholipids was observed after 11 days of dark stress, and this value was stable (~40%) for plants kept in the dark for up to 14 days. These results demonstrate that during dark stress PBM is degraded with, in parallel, a possible increase of its fluidity related to a higher unsaturation of the fatty acids. This suggests a probable impact on the regulation of metabolic exchanges between the cytoplasm of the nodular cells and bacteroids.

Discussion

The results presented in this article provide further evidence concerning strong metabolic and ultrastructural effects triggered by dark stress-induced senescence of nodules attached to soybean roots. For this purpose, NMR spectroscopy was used as a new approach to investigate the dynamics of nodule metabolism during senescence. Because symbiotic functioning in soybean nodules requires a flow of carbon representing 40% of that produced by photosynthesis, the first indication of the cessation of photosynthesis is the exhaustion of plant carbohydrate stores. Indeed, more than 80% of the sucrose was consumed inside nodules after 11 days in the dark, a result in agreement with Ching et al. (1975) and Pau and Cowles (1979). As well, a loss of 97% in sucrose content after 1 day of dark treatment was observed in indeterminate nodules (*P. sativum*, Matamoros et al. 1999). This phenomenon could be correlated with a decrease in the sucrose synthase activity and in the expression of its corresponding gene (Gordon et al. 1993; Van de Velde et al. 2006). Of particular interest is the

Table 2 Effects of dark stress on the fatty acid composition of PBM from soybean nodules

Days + 30 dpi	18:n/16:0 + 18:0		Proportion of fatty acids (% of total)									
			16:0		18:0		18:1		18:2		18:3	
	L	D	L	D	L	D	L	D	L	D	L	D
0	0.91	0.91	45.4 ± 4.6	45.4 ± 4.6	6.9 ± 0.4	6.9 ± 0.4	6.7 ± 0.5	6.7 ± 0.5	30.9 ± 2.8	30.9 ± 2.8	10.0 ± 1.0	10.0 ± 1.0
4	0.95	0.67	42.8 ± 1.3	44.0 ± 0.9	8.5 ± 0.4	15.7 ± 2.6	7.3 ± 0.3	5.9 ± 0.3	30.6 ± 1.3	26.1 ± 2.3	10.8 ± 0.7	8.3 ± 0.9
7	0.92	0.95	42.8 ± 0.2	41.5 ± 0.6	9.2 ± 0.5	9.7 ± 0.6	5.7 ± 0.4	5.5 ± 0.3	30.8 ± 1.0	33.2 ± 1.1	11.4 ± 0.2	10.2 ± 0.3
11	1.02	0.98	40.6 ± 0.8	39.0 ± 0.7	9.0 ± 0.6	11.4 ± 0.7	5.9 ± 0.3	6.3 ± 0.8	31.8 ± 0.2	34.1 ± 1.4	12.7 ± 0.2	9.2 ± 0.8
14	0.83	1.06	40.1 ± 0.9	36.8 ± 0.7	14.5 ± 0.8	11.7 ± 0.03	4.8 ± 0.1	5.2 ± 0.2	29.0 ± 1.1	35.6 ± 0.5	11.7 ± 0.1	10.7

The percentage of each fatty acid was calculated at the various stages of development described in Fig. 3. dpi, Days post-infection; L, control; D, dark treatment. 16:0, palmitic acid; 18:0, stearic acid; $16:1^{\Delta 3trans}$, palmitic acid; $18:1^{\Delta 9cis}$, oleic acid; $18:2^{\Delta 9,12}$, linoleic acid and $18:3^{\Delta 9,12,15}$, α-linolenic acid. Values represent the mean ± SD ($n = 3$)

detection of the second most abundant sugar, trehalose, only half of which is metabolised in senescing soybean nodules. Widely distributed in a large variety of prokaryotic and eukaryotic organisms (for a review, see Elbein et al. 2003), this disaccharide is however confined to Leguminosae only in soybean and French bean nodules (determinate nodules), which are colonised by their own rhizobia (Müller et al. 1994). In soybean nodules, trehalose is specifically synthesised in bacteroids and part of this sugar (34%) is released into the cytoplasm of nodule cells, where it plays a key role in the regulation of nodule carbohydrate by increasing sucrose breakdown (Streeter 1987; Müller et al. 1998). This strategy allows bacteroids to control their own carbon supply and hence N_2 assimilation but it also governs plant growth development (Rolland et al. 2006). However, in our assays the percentage of remaining trehalose detected in senescing nodules (53%) corresponds approximately to that present in bacteroids suggesting that only the pool of trehalose present in the nodule cells was probably used as a source of carbon because most of the trehalase (trehalose-cleaving enzyme) activity was localised in the cytosol (Streeter 1982).

Moreover, this process is accompanied by a decrease in key glycolytic metabolite intermediates such as Glc6P, Fru6P and DHAP, but also by the collapse of malate, one of the principal reductive final products of the glycolysis which supports N_2 assimilation in bacteroids (for a review see Lodwig and Poole 2003). This is consistent with the depletion of glutamine and asparagine concentrations, the two main amino acids assimilating NH_4^+, and with the disappearance of alanine which is considered as a possible alternative amino acid in N_2 fixation (for a review, see Day et al. 2001). Moreover, the accumulation of ureides observed in senescing nodules may be representative of the decrease in N_2 fixation. Indeed, King and Purcell (2005) demonstrated that the ureides may contribute to the feedback inhibition of nitrogenase activity specifically in soybean nodules. Furthermore, if we consider that the ureide accumulation coincides with the disappearance of nitrogenase transcripts, observed by Fargeix et al. (2004), after 11 days of dark treatment, it can be argued that there is a possible down-regulation of nitrogenase at the transcriptional levels by the ureides. Because ureides are exported from the nodules to the shoots where they are catabolised, we suggest that the accumulation of the ureides in senescing nodules can be attributed to water deficits and/or to the decrease in ureide catabolism in leaves (Vadez and Sinclair 2000, 2001). Alternately, it may also be the result of purine catabolism, because of a decrease by a factor of 3 in the level of NMP in senescing nodules (for a review, see Zrenner et al. 2006). Taken together, these results show that in the absence of a flow of photosynthate carbon, all the carbohydrate stores in the plant cell fraction of nodules are siphoned off as a consequence of a direct impact on nitrogen metabolism.

Simultaneously, with these metabolite consumptions, analysis of senescing soybean nodules by SEM shows cells filled with free intact bacteroids, which is a result of a desegregation of the symbiosome structure in infected cells, confirming results obtained using TEM by Cohen et al. (1986) and Fargeix et al. (2004). Considering that the total area of PBM per nodule is 20- to 100-fold that of the plasma membrane, its hydrolysis can provide a large amount of carbohydrates in a situation of carbon deprivation, such as is observed in senescing soybean nodules during dark stress. Correlatively, compounds liberated by phospholipid hydrolysis, like P-cho in the case of phosphatidylcholine, are accumulated in senescing tissues. Because of the huge accumulation of P-cho in dark stress nodules, it could be considered as a reliable marker of PBM lipid breakdown as observed by Roby et al. (1987) in *Acer pseudoplatanus* cells. Another evidence for PBM polar lipid catabolism is furnished by the accumulation in dark stress nodules of various glycerophosphodiesters [glycerylphosphoryl–inositol (GPI), glycerylphosphoryl–glycerol (GPG), glycerylphosphoryl–ethanolamine (GPE) and glycerylphosphoryl–choline (GPC)], which originate from the activity of non-specific lipolytic acyl-hydrolases (Galliard 1980). In addition, the accumulation of Glyc3P and free choline in dark stress nodules suggests that GPC is also hydrolysed. Under this condition, Glyc3P can be utilised like fatty acids as an energy substrate by nodule cells, such as observed in sucrose-deprived sycamore and carrot cells (Aubert et al. 1996; Van der Rest et al. 2002). Thus, our results indicate that the hydrolysed PBM lipids may serve as a reserve of carbohydrate, an event which can be correlated with the (re)-initiation of the host-cell glyoxylate cycle observed by Fargeix et al. (2004). The transition from sugar to lipid membrane as a source of nutrient was also observed in indeterminate nodules (*M. truncatula*) via the expression of a number of catabolic genes (Van de Velde et al. 2006). This suggests that all types of senescing nodules probably use a common mechanism to provide nodule cells with the energy required for ATP and NADPH synthesis via the dismantling of symbiosomes. In untreated nodules, we observe a very high AMP/ATP ratio (12.6), which is an indicator of a hypoxic metabolism because, to avoid nitrogenase injury, legume nodules maintain a very low tension of O_2 in infected cells (5–50 nM), explaining the limited yield of ATP synthesis (Kuzma et al. 1999). When soybeans suffer dark treatment for 11 days, the AMP/ATP ratio (5.4) decreases because of the threefold decrease in AMP, but not to the level of ATP, which remains approximately constant. This suggests that a significant part of the acyl residues deriving from PBM catabolism yields energy to maintain respiration. However, during PBM dismantling,

H_2O_2 was probably generated by β-oxidation of fatty acids (for a review see Vauclare et al. 2003). Indeed, GABA accumulation in senescing nodules could reflect an increase in hypoxic conditions, an acidification of cytosolic pH and an increase in the oxidative stress (for a review, see Bouché and Fromm 2004). This suggests that nodules' cells need to increase their anti-oxidant defence. However, we observed an accumulation of NADP and Glcn6P in senescing nodules, which indicates a diminution of the production of reducing power in nodules via the pentose phosphate pathway, a situation which favours oxidative stress because the ascorbate–glutathione cycle, which is the main anti-oxidant defence of nodules, needs NADPH to work (Dalton et al. 1986). The diminution in the level of the ascorbate precursor, mannose 6-phosphate (Man6P), in senescing nodules may also affect the ascorbate biosynthetic pathway and, subsequently, the nodule anti-oxidant defence capacities as observed in indeterminate nodules (*P. sativum*) by Matamoros et al. (1999). Consequently, this constitutes a risk for PBM lipid peroxidation by reactive oxygen species (ROS; for a review, see Puppo et al. 2005). In addition, the two PBM unsaturated fatty acids (oleic and linoleic acid) from 11 days of darkness could enhance fatty acid peroxidation. This is considered by Puppo et al. (1991) as one of the major events involved in the modification of PBMs' permeability and their eventual rupture, with a direct effect on symbiosis.

To summarise, the present study reveals that dark-induced senescence in soybean triggers a complex process of autophagy at the level of symbiosomes, which could physiologically mimic programmed cell death. This process starts with the exhaustion of the reserve carbohydrates followed by a decrease in primary metabolism, a collapse of the nitrogen metabolism and PBM phospholipid hydrolysis, which release substrates required to maintain a minimum physiological activity. The decrease of anti-oxidant capacities in the nodules makes it easier for ROS to break down the PBM, suggesting that, once the autophagic process is started in senescing nodules, the process become autocatalytic. Because of the key properties of the PBM in symbiosis (for a review, see Udvardi and Day 1997), its hydrolysis during senescence probably cuts off the symbiotic relationship established between the plant and the microsymbionts. For this reason and on the basis of the result obtained by Werner et al. (1985), we can speculate that bacteroids released in the host cytoplasm could be recognised as parasites by the senescing plant. Further analyses are required to provide greater insight into the metabolic adaptation of the bacteroids and nodule host cells of soybean when symbiosis is broken off. Likewise, it will be important to establish whether the autophagic process induced in the dark can be reversed in stressed nodules.

Acknowledgments We are grateful to Dr. John Lomas (ITODYS UMR 7086, Université Paris-Diderot, Paris 7) for his fine work in correction of English text in the manuscript. We also thank Josiane Bonetti for her excellent bibliographic assistance. This work was supported by grants from the University of Lausanne (Switzerland).

References

Andreeva IN, Kozharinova GM, Izmailov SF (1998) Senescence of legume nodules. Russ J Plant Physiol 45:101–112

Anthon GE, Emerich DW (1990) Developmental regulation of enzymes of sucrose and hexose metabolism in effective and ineffective soybean nodules. Plant Physiol 92:346–351

Aubert S, Gout E, Bligny R, Marty-Mazars D, Barrieu F, Alabouvette J, Marty F, Douce R (1996) Ultrastructural and biochemical characterization of autophagy in higher plant cells subjected to carbon deprivation: control by supply of mitochondria with respiratory substrates. J Cell Biol 133:1251–1263

Bassarab S, Schenk SU, Werner D (1989) Fatty acid composition of the peribacteroid membrane and the ER in nodules of *Glycine max* varies after infection by different strains of the microsymbiont *Bradyrhizobium japonicum*. Bot Acta 102:196–201

Bligh EG, Dyer WJ (1959) A rapid method of total lipid extraction and purification. Can J Biochem Physiol 37:911–917

Bouché N, Fromm H (2004) GABA in plants: just a metabolite? Trends Plant Sci 9:110–115

Broughton WJ (2003) Roses by other names: taxonomy of the *Rhizobiaceae*. J Bacteriol 185:2975–2979

Ching TM, Hedtke S, Russel SA, Evans HJ (1975) Energy state and dinitrogen fixation in soybean nodules of dark-grown plants. Plant Physiol 55:796–798

Cohen HP, Sarath G, Lee K, Wagner FW (1986) Soybean root nodule ultrastructure during dark-induced stress and recovery. Protoplasma 132:69–75

Cots J, Fargeix C, Gindro K, Widmer F (2002) Pathogenic attack and carbon reallocation in soybean leaves (*Glycine max* L.): reinitiation of the glycoxylate cycle as a defense reaction. J Plant Physiol 159:91–96

Dalton DA, Russell SA, Hanus FJ, Pascoe GA, Evans HJ (1986) Enzymatic reactions of ascorbate and glutathione that prevent peroxide damage in soybean root nodules. Proc Natl Acad Sci USA 83:3811–3815

Day DA, Copeland L (1991) Carbon metabolism and compartmentation in nitrogen-fixing legume nodules. Plant Physiol Biochem 29:185–201

Day DA, Price GD, Gresshof PM (1987) A comparison of mitochondria from soybean nodules, roots and cotyledons. In: Moore AL, Beechey RB (eds) Plant mitochondria: structural, functional and physiological aspects. Plenum Press, New York, pp 207–210

Day DA, Poole PS, Tyerman SD, Rosendahl L (2001) Ammonia and amino acid transport across symbiotic membranes in nitrogen-fixing legume nodules. Cell Mol Life Sci 58:61–71

Dorne A-J, Bligny R, Rébeillé F, Roby C, Douce R (1987) Fatty acid disappearance and phosphorylcholine accumulation in higher plant cells after a long period of sucrose deprivation. Plant Physiol Biochem 25:589–595

Doyle JJ, Luckow MA (2003) The rest of the iceberg Legume diversity and evolution in a phylogenetic context. Plant Physiol 131:900–910

Elbein AD, Pan YT, Pastuszak I, Carroll D (2003) New insights on trehalose: a multifunctional molecule. Glycobiology 13(4):17R–27R

Espinosa-Victoria D, Vance CP, Graham PH (2000) Host variation in traits associated with crown nodule senescence in soybean. Crop Sci 40:103–109

Fargeix C, Gindro K, Widmer F (2004) Soybean (*Glycine max* L.) and bacteroid glyoxylate cycle activities during nodular senescence. J Plant Physiol 161:183–190

Galliard T (1980) Degradation of acyl lipids: hydrolytic and oxidative enzymes. In: Stumpf PK (ed) The biochemistry of plants. A comprehensive treatise, vol 4. Academic Press, New York, pp 85–116

Gordon AJ, Ougham HJ, James CL (1993) Changes in the levels of gene transcripts and their corresponding proteins in nodules of soybean plant subjected to dark-induced stress. J Exp Bot 44:1453–1460

Gout E, Aubert S, Bligny R, Rébeillé F, Nonomura AR, Benson AA, Douce R (2000) Metabolism of methanol in plant cells. Carbon-13 nuclear magnetic resonance studies. Plant Physiol 123:287–296

Hong ZQ, Copeland L (1990) Pentose phosphate pathway enzymes in nitrogen-fixing leguminous root nodules. Phytochemistry 29:2437–2440

Jacobi A, Katinakis P, Werner D (1994) Artificially induced senescence of soybean root nodules affects different polypeptides and nodulins in the symbiosome membrane compared to physiological ageing. J Plant Physiol 144:533–540

King CA, Purcell LC (2005) Inhibition of N_2 fixation in soybean is associated with elevated ureides and amino acids. Plant Physiol 137:1389–1396

Kuzma MM, Winter H, Storer P, Oresnik II, Atkins CA, Layzell DB (1999) The site of oxygen limitation in soybean nodules. Plant Physiol 119:399–408

Lee JW, Zhang Y, Weaver CD, Shomer NH, Louis CF, Roberts DM (1995) Phosphorylation of nodulin 26 on serine 262 affects its voltage-sensitive channel activity in planar lipid bilayers. J Biol Chem 270:27051–27057

Lodwig E, Poole P (2003) Metabolism of *Rhizobium* bacteroids. Crit Rev Plant Sci 22:37–78

Lord JM (1987) Isolation of endoplasmic reticulum: general principles, enzymatic markers, and endoplasmic reticulum bound polysomes. Methods Enzymol 148:576–584

Matamoros MA, Baird LM, Escurado PR, Dalton DA, Minchin FR, Iturbe-Ormaetxe I, Rubio MC, Moran JF, Gordon AJ, Becana M (1999) Stress-induced legume root nodule senescence physiological, biochemical, and structural alteration. Plant Physiol 121:97–111

Matamoros MA, Loscos J, Coronado MJ, Ramos J, Sato S, Testillano PS, Tabata S, Becana M (2006) Biosynthesis of ascorbic acid in legume root nodules. Plant Physiol 141:1068–1077

Miao GH, Verma DP (1993) Soybean nodulin-26 gene encoding a channel protein is expressed only in the infected cells of nodules and is regulated differently in roots of homologous and heterologous plants. Plant Cell 5:781–794

Müller J, Xie Z-P, Staehelin C, Mellor RB, Boller T, Wiemken A (1994) Trehalose and trehalase in root nodules from various legumes. Physiol Plant 90:86–92

Müller J, Boller T, Wiemken A (1998) Trehalose affects sucrose synthase and invertase activities in soybean (*Glycine max* [L.] Merr.) roots. J Plant Physiol 153:255–257

Newton WE (2000) Nitrogen fixation. In: Pedrosa FO, Hungria M, Yates MG, Newton WE (eds) From molecules to crop productivity. Kluwer, Dordrecht, pp 3–8

Patriarca EJ, Tate R, Ferraioli S, Laccarino M (2004) Organogenesis of legume root nodules. Int Rev Cytol 234:201–262

Pau AS, Cowles JR (1979) Effect of induced nodule senescence on parameters related to dinitrogen fixation, bacteroid size, and nucleic acid content. J Gen Microbiol 111:101–107

Perret X, Staehelin C, Broughton WJ (2000) Molecular basis of symbiotic promiscuity. Microbiol Mol Biol Rev 64:180–201

Pfeiffer NE, Malik NSA, Wagner FW (1983) Reversible dark-induced senescence of soybean root nodules. Plant Physiol 71:393–399

Prell J, Poole P (2006) Metabolic changes of rhizobia in legume nodules. Trends Microbiol 14:1–8

Puppo A, Herrada G, Rigaud J (1991) Lipid peroxidation in peribacteroid membrane from French bean nodules. Plant Physiol 96:826–830

Puppo A, Groten K, Bastian F, Carzaniga R, Soussi M, Mercedes Lucas M, Rosaria de Felipe M, Harisson J, Vanacker H, Foyer CH (2005) Legume nodule senescence: roles for redox and hormone signalling in the orchestration of the natural aging process. New Phytol 165:683–701

Quail PH (1979) Plant cell fractionation. Annu Rev Plant Physiol 30:425–484

Roby C, Martin JB, Bligny R, Douce R (1987) Biochemical changes during sucrose deprivation in higher plant cells. Phosphorus-31 nuclear magnetic resonance studies. J Biol Chem 262:5000–5007

Rolland F, Baeana-Gonzalez E, Sheen J (2006) Sugar sensing and signalling in plants: conserved and novel mechanisms. Annu Rev Plant Biol 57:675–709

Schubert KR (1986) Products of biological nitrogen fixation in higher plants; synthesis, transport and metabolism. Annu Rev Plant Physiol 37:539–574

Streeter JG (1982) Enzymes of sucrose, maltose and alpha, alpha-trehalose catabolism in soybean root nodules. Planta 155:112–115

Streeter JG (1987) Carbohydrate, organic acid, and amino acid composition of bacteroids and cytosol from soybean nodules. Plant Physiol 85:768–773

Tajima S, Nomura M, Kouchi H (2004) Ureide biosynthesis in legume nodules. Front Biosci 9:1374–1381

Udvardi MK, Day DA (1997) Metabolite transport across symbiotic membranes of legume nodules. Annu Rev Plant Physiol Plant Mol Biol 48:493–523

Vadez V, Sinclair TR (2000) Ureide degradation pathways in intact soybean leaves. J Exp Bot 51:1459–1465

Vadez V, Sinclair TR (2001) Leaf ureide degradation and N_2 fixation tolerance to water deficit in soybean. J Exp Bot 52:153–159

Van de Velde W, Pérez Guerra JC, De Keyser A, De Rycke R, Rombauts S, Maunoury N, Mergaert P, Kondorosi E, Holsters M, Goormachtig S (2006) Aging in legume symbiosis A molecular view on nodule senescence in Medicago truncatula. Plant Physiol 141:711–720

Van der Rest B, Boisson A-M, Gout E, Bligny R, Douce R (2002) Glycerophosphocholine metabolism in higher plant cells evidence of a new glyceryl-phosphodiester phosphodiesterase. Plant Physiol 130:244–255

Vauclare P, Cots J, Gindro K, Widmer F (2003) The glyoxylate cycle as an essential step in carbon reallocation mechanisms. Adv Plant Physiol 5:97–132

Weaver CD, Crombie B, Stacey G, Roberts DM (1991) Calcium-dependent phosphorylation of symbiosome membrane proteins from nitrogen-fixing soybean nodules: evidence for phosphorylation of Nodulin-26. Plant Physiol 95:222–227

Werner D, Mellor RB, Hahn MG, Grisebach H (1985) Soybean root response to symbiotic infection Glyceollin I accumulation in an ineffective type of soybean nodules with an early loss of the peribacteroid membrane. Z Naturfosch 40:179–181

Wheeler GL, Jones MA, Smirnoff N (1998) The biosynthetic pathway of vitamin C in higher plants. Nature 393:365–369

Zrenner R, Stitt M, Sonnewald U, Boldt R (2006) Pyrimidine and purine biosynthesis and degradation in plants. Annu Rev Plant Biol 57:805–836